SIMPLIFIED TRANSIENT TWO-PHASE MODEL FOR PIPE FLOW

Olusola Oloruntoba, Cranfield University; Fuat Kara, Cranfield University

Abstract

Two-phase flow analyses are critical to successful design and operations of two-phase and multiphase pipe flow applications found in major industrial fields, such as petroleum, nuclear, chemical, geothermal and space industries. Due to difficulties in obtaining analytical transient solutions, approximate solutions have been applied to two-phase pipe flow. However, these approximate solutions neglect convective terms in two-phase Navier-Stokes equations. The aim of this current study was to develop transient tools to predict transient two-phase pipe flow. The objectives of this study were to develop a simplified transient model and to validate the proposed model with published experimental data. A simplified transient two-phase pipe flow model was obtained in this study by simplifying the two-phase Navier-Stokes equations. The simplified equations include: (i) a transient continuity equation of combined two-phase flow that includes two new dimensionless terms; (ii) transient two-phase momentum equations that account for convective terms only; and, (iii) a steady state pressure gradient.

Introduction

Multiphase flow occurs in major industrial fields, including the petroleum, chemical, geothermal, nuclear, and space industries. Steady state and transient prediction models are required for adequate design of these multiphase applications in these industries [1, 2]. Unfortunately, rigorous analytical solutions are limited to but a few flow scenarios. Numerical methods provide approximate solutions but are limited, due to high demand for computational time and resources; especially for transient simulations [3]. Mechanistic methods, which rely on physical analyses based on flow pattern, have been successfully applied for steady state flows [1]. Therefore, simplified transient models have been sought after to achieve fast transient simulators.

Taitel et al. [4] proposed a simplified transient two-phase model that treats liquid continuity as the only transient equation; momentum equations for gas and liquid, and a gas continuity equation were treated in a quasi-steady state. These assumptions are valid for slow transient flow variations. The model of Taitel et al. was modified by Minami and Shoham [5] using an implicit scheme instead of an explicit scheme implemented in the original model. Minami and Shoham also developed a new flow regime transition model for transient flow. The modified model from Taitel et al. was tested against experimental data collected in a 420m long and 7.79 cm diameter pipe, in an air-kerosene two-fluid system. The validation results showed good agreement between their model and the experimental data, with the exception of the liquid blowdown test. During the liquid blowdown test, when the liquid flow rate is set to zero with the gas flow rate sustained, complete liquid removal was not achieved. Li [6] developed a simplified two-phase transient model by treating continuity equations as transient, but with momentum equations in a quasi-steady state. Li validated this model using the data from Vigneron et al. [7]. Later, Choi et al. [8] developed a simplified transient two-phase model to solve modified continuity equations, but treated momentum equations as an extended drift flux equation in the quasi-steady state.

Existing simplified transient models assume complete quasi-steady state conditions for momentum equations. Consequently, an alternative simplified transient two-phase model can be developed by considering convective terms in momentum equations, as well as continuity equations in the transient state. This alternative simplified transient model was developed in this study.

Model Description

Navier-Stokes Equations

One-dimensional two-phase Navier-Stokes equations [3], with negligible contribution from the energy equation and mass transfer between the phases, were considered and are presented in the continuity equations of Equations (1) and (2), and the momentum equations of Equations (3) and (4):

$$\frac{\partial}{\partial t}\left(\rho_G \alpha_G\right)+\frac{\partial}{\partial x}\left(\rho_G \alpha_G U_G\right)=0 \tag{1}$$

$$\frac{\partial}{\partial t}\left(\rho_L \alpha_L\right)+\frac{\partial}{\partial x}\left(\rho_L \alpha_L U_L\right)=0 \tag{2}$$

$$\begin{aligned}&\frac{\partial}{\partial t}\left(\rho_G \alpha_G U_G\right)+\frac{\partial}{\partial x}\left(\rho_G \alpha_G U_G^2\right)\\&=-\alpha_G \frac{\partial P_G}{\partial x}-\tau_{GW}-\tau_{GL}-\alpha_G \rho_G g \sin\theta\end{aligned} \tag{3}$$

$$\frac{\partial}{\partial t}\left(\rho_L \alpha_L U_L\right)+\frac{\partial}{\partial x}\left(\rho_L \alpha_L U_L^2\right) = -\alpha_L \frac{\partial P_L}{\partial x}-\tau_{LW}+\tau_{GL}-\alpha_L \rho_L g \sin\theta \quad (4)$$

Modified Navier-Stokes Equations

The Navier-Stokes equations presented in Equations (1)-(4) consist of four equations, with eight unknown variables, namely: ρ_G, ρ_L, α_G, α_L, U_G, U_L, P_G, and P_L. To simplify the Navier-Stokes, and to achieve zero degrees of freedom, the following modifications were introduced.

Modifications introduced from previous studies:

- Incompressible flow was assumed [3]
- Superficial velocities are defined as $U_{SG} = \alpha_G U_G$ and $U_{SL} = \alpha_L U_L$ [1]
- Steady state pressure gradient was assumed (valid for slowly varying flow, such as in the petroleum industry [1])
- Single pressure applies to gas and liquid by $P_G = P_L = P$ [9]
- Summation of phase fractions is unity, given as $\alpha_G + \alpha_L = 1$ [3]

Modifications introduced in this study:

- In this study, the average of Equations (1) and (2) was determined in order to obtain a combined continuity equation; noting that incompressibility was assumed and that $\alpha_G = 1 - \alpha_L$.
- Two new dimensionless terms, α_L / H_L and $(1 - \alpha_L)/(1 - H_L)$, were introduced in the combined continuity equation. This was aimed at introducing transient liquid holdup dependence on liquid holdup distribution along the length of the pipe. The dimensionless terms represent ratio of transient phase fraction to steady state phase fraction. Theoretically, these terms should converge to unity, as transient simulations approach steady state conditions.
- Convective terms in the momentum equations—Equations (3)-(4)—were retained as part of the simplified transient model.

Application of these modifications to Equations (1)-(4) yields the simplified transient two-phase model, as presented by the combined continuity equation of Equation (5) and the simplified momentum equations of Equations (6) and (7):

The conservation variables are α_L, U_{SG}, and U_{SL}.

$$\frac{\partial}{\partial t}\left(\alpha_L\right)-\frac{1}{2\rho_G}\frac{\partial}{\partial x}\left\{\left(\frac{1-\alpha_L}{1-H_L}\right)\rho_G U_{SG}\right\}+\frac{1}{2\rho_L}\frac{\partial}{\partial x}\left\{\left(\frac{\alpha_L}{H_L}\right)\rho_L U_{SL}\right\}=0 \quad (5)$$

$$\frac{\partial}{\partial t}\left(U_{SG}\right)+\frac{1}{\rho_G}\frac{\partial}{\partial x}\left\{\left(\frac{\rho_G}{1-\alpha_L}\right)U_{SG}^2\right\}=0 \quad (6)$$

$$\frac{\partial}{\partial t}\left(U_{SL}\right)+\frac{1}{\rho_L}\frac{\partial}{\partial x}\left\{\left(\frac{\rho_G}{\alpha_L}\right)U_{SL}^2\right\}=0 \quad (7)$$

where, the steady state pressure gradient equations are given in Equations (8) and (9).

$$-\frac{dP}{dx}=\frac{2 f_m \rho_m U_m^2}{D} \quad (8)$$

$$f_m = F_2 + \frac{F_1 - F_2}{\left[1+\left(\frac{Re}{t^*}\right)^c\right]^d} \quad (9)$$

Equation (8) expresses the steady state pressure gradient model of García et al. [10]. The model of Garcia et al. was employed for its simplicity and applicability to all flow regimes [8]. The friction factor, f_m, is given in Equation (9). The authors defined the following power laws: $F_1 = a_1 Re^{b1}$ and $F_2 = a_2 R^{b2}$; Reynold's number of mixture flow $Re = U_m D/\nu_L$; mixture velocity $U_m = U_{SG} + U_{SL}$; mixture density $\rho_m = \rho_L \lambda_L + \rho_G(1 - \lambda_L)$; and, kinematic viscosity of liquid $\nu_L = \mu_L/\rho_L$. Coefficients a_1, b_1, a_2, b_2, c, d, and t^* are defined as 13.98, -0.9501, 0.0925, -0.2534, 4.864, 0.1972, and 293, respectively.

Steady state liquid holdup, H_L, was calculated iteratively using Equation (10) and the method of Choi et al. [11]. An initial guess value of $\alpha_G = 0.5$ was applied. At subsequent iteration steps, $\alpha_G = 1 - H_L$. The distribution parameter, C_0, is given in Equation (11):

$$H_L = 1 - \frac{U_{SG}}{C_0 U_m + U_D} \quad (10)$$

$$C_0 = \frac{2}{1+\left(\frac{Re}{1000}\right)^2}+\frac{1.2-0.2\sqrt{\frac{\rho_G}{\rho_L}}\left(1-exp\left(-18\alpha_G\right)\right)}{1+\left(\frac{1000}{Re}\right)^2} \quad (11)$$

Drift velocity, U_D, is given in Equation (12):

$$U_D = A\cos\theta + B\left(\frac{g\sigma\left(\rho_L-\rho_G\right)}{\rho_L^2}\right)^{1/4}\cos\theta \quad (12)$$

where, $Re = \rho_L U_m D/\mu_L$ is the Reynold's number and coefficients A and B are given as 0.0246 and 1.606, respectively.

Validation of Steady State Equations

The steady state pressure gradient of Equation (8) was validated using published experimental data [12-15]. The data of Asante [12] consisted of 255 and 243 data points of stratified and annular/mist flow regime, respectively. The experiment was carried out for an oil-water-air flow in a horizontal pipe with a diameter range of 0.0254m - 0.0762m at standard conditions. A total of 38 slug flow data points were obtained from Hernandez [13]. The experiment of Hernandez was carried out for water-air flow in a 0.038m diameter pipe, inclined between 0° and 90°. The data of Marruaz et al. [14] consisted of 23 data points of slug flow regime. The experiment of Marruaz et al. was carried out for oil-water-gas flow in a 0.15m diameter horizontal pipe. The data obtained from Tullius [15] consisted of 101 data points of slug flow regime. The experiment of Tullius was conducted for oil-water-air flow in a 0.101m diameter horizontal pipe.

The average percentage of error is defined in Equation (13):

$$\varepsilon_{ave} = \left(\frac{experimental\ data - prediction}{prediction} \right) \times 100\ \% \qquad (13)$$

Figure 1 shows that the validation results from Equation (8) predict 83% of experimental pressure gradient data within $-30\% \le \mathring{a}_{ave} \le +30\%$.

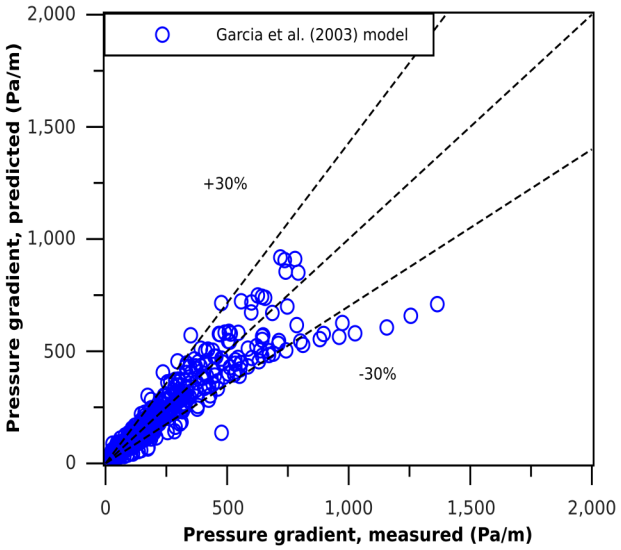

Figure 1. Validation of the Steady State Pressure Gradient Model Given in Equation (8)

Numerical Discretization

The proposed simplified transient two-phase model was discretized using a finite volume upwind scheme, with a scattered grid arrangement in the spatial domain. Time marching was implemented explicitly. Equation (14) is the combined continuity equation. Equations (15) and (16) are the simplified momentum equations of gas and liquid, respectively. Slope limiter, β, was defined for gas and liquid velocities at computational nodes in order to determine flow directions [3]. For example, gas slope limiter at volume node $(i + 1/2)$ was defined as

$$\beta^G_{i+1/2} = \left(U_{SG}\right)^n_{i+1/2} \Big/ \left|\left(U_{SG}\right)^n_{i+1/2}\right|$$

$$\begin{aligned} &\frac{\left(\alpha_L\right)^{n+1}_i - \left(\alpha_L\right)^n_i}{\Delta t} = \\ &A_1\left(\left(U_{SG}\right)^n_{i-\frac{1}{2}}\left[1-\left(\alpha_L\right)^n_{i-1}\right]\right) \\ &+A_2\left(\left(U_{SG}\right)^n_{i+\frac{1}{2}}\left[1-\left(\alpha_L\right)^n_{i}\right]\right) \\ &+A_3\left(\left(U_{SL}\right)^n_{i-\frac{1}{2}}\left(\alpha_L\right)^n_{i-1}\right) \\ &+A_4\left(\left(U_{SL}\right)^n_{i+\frac{1}{2}}\left(\alpha_L\right)^n_{i}\right) \end{aligned} \qquad (14)$$

where,

$$A_1 = \left(\frac{1}{2\rho_G}\right)^n_i \left(\frac{-1}{\Delta x}\right)_i \left\{\left(\frac{1+\beta^G_{i-\frac{1}{2}}}{2}\right)\left(\frac{\rho_G}{1-H_L}\right)_{i-1} + \left(\frac{1-\beta^G_{i-\frac{1}{2}}}{2}\right)\left(\frac{\rho_G}{1-H_L}\right)_i\right\}^n$$

$$A_2 = \left(\frac{1}{2\rho_G}\right)^n_i \left(\frac{1}{\Delta x}\right)_i \left\{\left(\frac{1+\beta^G_{i+\frac{1}{2}}}{2}\right)\left(\frac{\rho_G}{1-H_L}\right)_{i} + \left(\frac{1-\beta^G_{i+\frac{1}{2}}}{2}\right)\left(\frac{\rho_G}{1-H_L}\right)_{i-1}\right\}^n$$

$$A_3 = \left(\frac{1}{2\rho_L}\right)^n_i \left(\frac{1}{\Delta x}\right)_i \left\{\left(\frac{1+\beta^L_{i-\frac{1}{2}}}{2}\right)\left(\frac{\rho_L}{H_L}\right)_{i-1} + \left(\frac{1-\beta^L_{i-\frac{1}{2}}}{2}\right)\left(\frac{\rho_L}{H_L}\right)_i\right\}^n$$

$$A_4 = \left(\frac{1}{2\rho_L}\right)^n_i \left(\frac{-1}{\Delta x}\right)_i \left\{\left(\frac{1+\beta^L_{i+\frac{1}{2}}}{2}\right)\left(\frac{\rho_L}{H_L}\right)_{i} + \left(\frac{1-\beta^L_{i+\frac{1}{2}}}{2}\right)\left(\frac{\rho_L}{H_L}\right)_{i-1}\right\}^n$$

$$\begin{aligned} &\frac{\left(U_{SG}\right)^{n+1}_{i+\frac{1}{2}} - \left(U_{SG}\right)^n_{i+\frac{1}{2}}}{\Delta t} = B_1\left\{\frac{\left[\left(U_{SG}\right)^n_{i-\frac{1}{2}}\right]^2}{1-\left(\alpha_L\right)^n_{i-\frac{1}{2}}}\right\} \\ &+B_2\left\{\frac{\left[\left(U_{SG}\right)^n_{i+\frac{1}{2}}\right]^2}{1-\left(\alpha_L\right)^n_{i+\frac{1}{2}}}\right\} + B_3\left\{\frac{\left[\left(U_{SG}\right)^n_{i+\frac{3}{2}}\right]^2}{1-\left(\alpha_L\right)^n_{i+\frac{3}{2}}}\right\} \end{aligned} \qquad (15)$$

where,

$$B_1 = \left(\frac{1}{\rho_G}\right)^n_{i+\frac{1}{2}} \left(\frac{1}{\Delta x}\right)_{i+\frac{1}{2}} \left\{\left(\frac{1+\beta^G_{i+\frac{1}{2}}}{2}\right)(\rho_G)_{i-\frac{1}{2}}\right\}^n$$

$$B_2 = \left(\frac{1}{\rho_G}\right)^n_{i+\frac{1}{2}} \left(\frac{-1}{\Delta x}\right)_{i+\frac{1}{2}} \left\{\beta^G_{i+\frac{1}{2}}(\rho_G)_{i+\frac{1}{2}}\right\}^n$$

$$B_3 = \left(\frac{1}{\rho_G}\right)^n_{i+\frac{1}{2}} \left(\frac{-1}{\Delta x}\right)_{i+\frac{1}{2}} \left\{\left(\frac{1-\beta^G_{i+\frac{1}{2}}}{2}\right)(\rho_G)_{i+\frac{3}{2}}\right\}^n$$

$$\frac{(U_{SL})^{n+1}_{i+\frac{1}{2}} - (U_{SL})^n_{i+\frac{1}{2}}}{\Delta t} = C_1 \left\{\frac{\left[(U_{SL})^n_{i-\frac{1}{2}}\right]^2}{(\alpha_L)^n_{i-\frac{1}{2}}}\right\} + C_2 \left\{\frac{\left[(U_{SL})^n_{i+\frac{1}{2}}\right]^2}{(\alpha_L)^n_{i+\frac{1}{2}}}\right\} + C_3 \left\{\frac{\left[(U_{SL})^n_{i+\frac{3}{2}}\right]^2}{(\alpha_L)^n_{i+\frac{3}{2}}}\right\} \quad (16)$$

where,

$$C_1 = \left(\frac{1}{\rho_L}\right)^n_{i+\frac{1}{2}} \left(\frac{1}{\Delta x}\right)_{i+\frac{1}{2}} \left\{\left(\frac{1+\beta^L_{i+\frac{1}{2}}}{2}\right)(\rho_L)_{i-\frac{1}{2}}\right\}^n$$

$$C_2 = \left(\frac{1}{\rho_L}\right)^n_{i+\frac{1}{2}} \left(\frac{-1}{\Delta x}\right)_{i+\frac{1}{2}} \left\{\beta^L_{i+\frac{1}{2}}(\rho_L)_{i+\frac{1}{2}}\right\}^n$$

$$C_3 = \left(\frac{1}{\rho_L}\right)^n_{i+\frac{1}{2}} \left(\frac{-1}{\Delta x}\right)_{i+\frac{1}{2}} \left\{\left(\frac{1-\beta^L_{i+\frac{1}{2}}}{2}\right)(\rho_L)_{i+\frac{3}{2}}\right\}^n$$

Pipe Geometry and Discretization

Figure 2 shows how the pipe profile was supplied as pipe segments based on pipe inclination angle. Each segment was discretized into elements, such that a uniform grid was obtained.

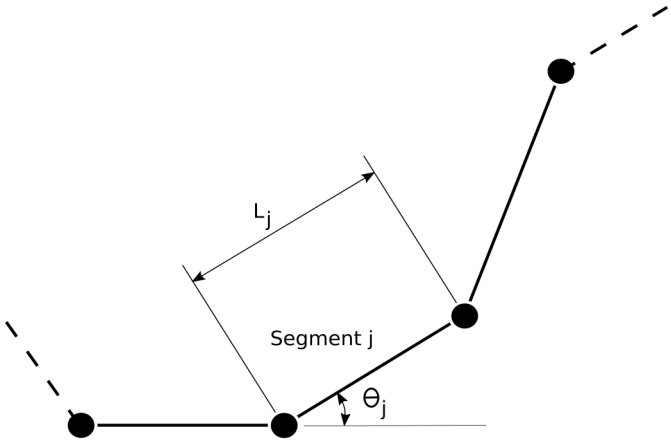

Figure 2. Pipe Profile Divided into Segments: L_j = Length of Segment j[*m*]; θ_j = Inclination Angle of Segment j[*degree*]

Boundary Conditions

Figure 3 depicts the computational domain and boundary conditions for the simplified transient two-phase model. The computational domain was $0 \le x \le L$. The inlet and outlet boundaries were given for (α_L, U_{SG}, U_{SL}) at $x = 0$, and for (P) at $x = L$, respectively. Ghost cells are generally required to estimate conservation variables at the boundaries [3].

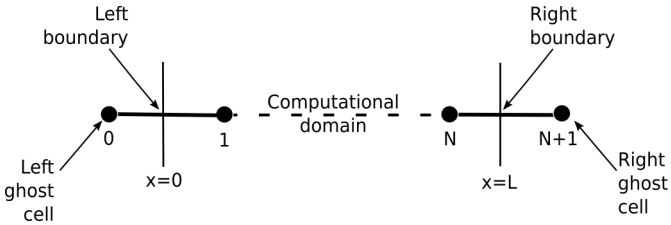

Figure 3. Computational Domain and Boundary Conditions

Sensitivity Analysis

Spatial and temporal sensitivity analyses were carried out for pressure gradient predictions using the proposed simplified transient two-phase model. For the spatial sensitivity analysis, the percentage of relative error was calculated relative to pressure drop at $N + 1 = 656$. For the temporal sensitivity analysis, the computational time ratio was calculated as $t_{ratio} = t_{N+1}/t_{42}$. Figures 4 and 5 present results of the spatial and temporal sensitivity analyses, respectively.

Validation of the Simplified Transient Two-Phase Model

The simplified transient two-phase model proposed in this study was validated using experimental data from Vigneron et al. [7]. The experiment of Vigneron et al. was carried out

in a 0.0779m diameter, 420m long horizontal steel pipeline, using an air-kerosene fluid system. The test station was at 61.4m from the air-kerosene mixing point.

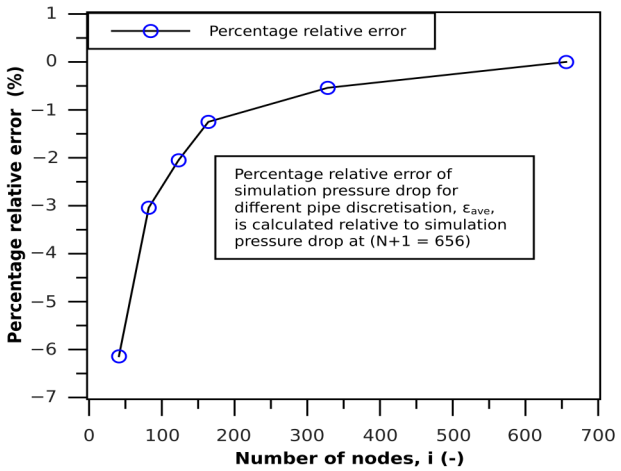

Figure 4. Sensitivity Analysis for the Spatial Steady State Pressure Gradient

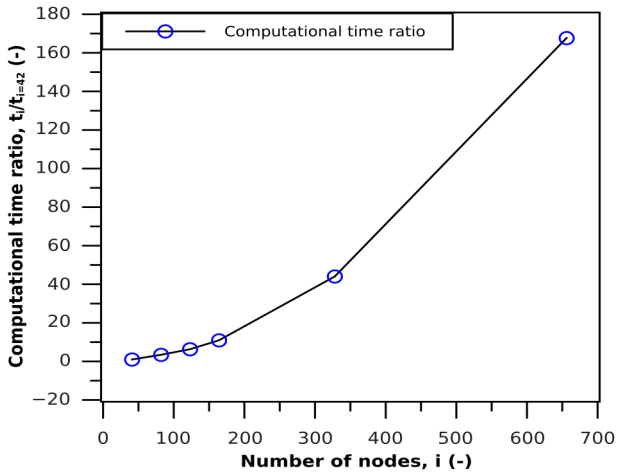

Figure 5. Sensitivity Analysis for the Temporal Steady State Pressure Gradient

Two test cases were used for validation. The first test case (Test 1-B) was at a gas flow rate of 400 Sm^3/d and consisted of initial and final liquid flows rate at 8.4 m^3/d and 31.8 m^3/d, respectively. The corresponding initial and final flow regimes were stratified smooth and stratified wavy, respectively. The second test case (Test 1-C) was at a gas flow rate of 4055 Sm^3/d and consisted of initial and final liquid flow rates at 8.4 m^3/d and 32 m^3/d, respectively. The stratified wavy flow regime was observed for the initial and final liquid flow rates.

Transient Algorithm

Figure 6 shows the algorithm for implementing the simplified transient two-phase model.

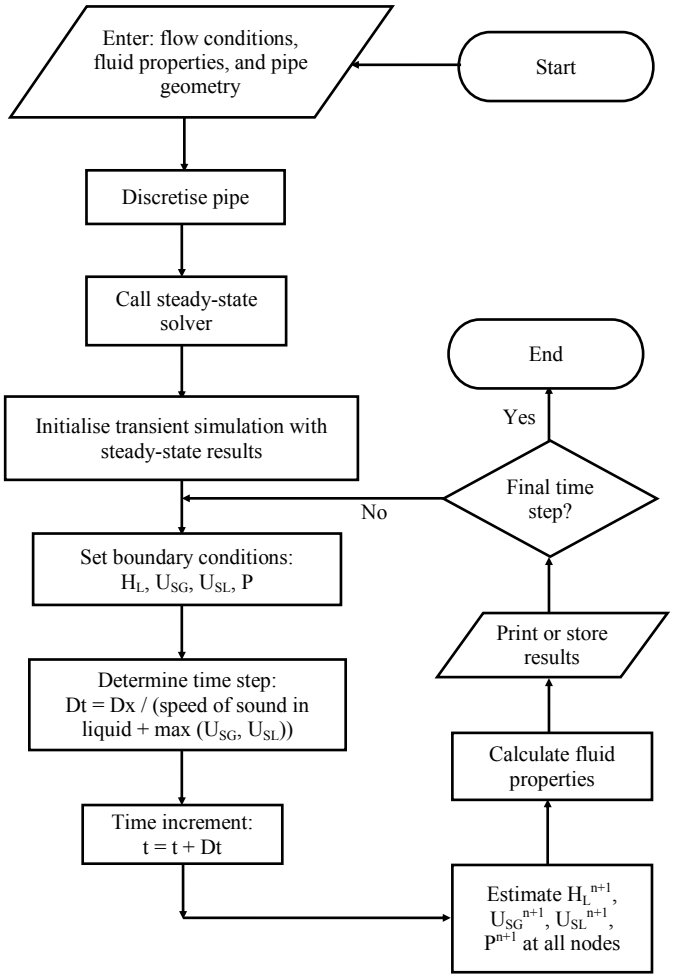

Figure 6. Algorithm for the Simplified Transient Two-Phase Model

Results and Discussion

Figures (7)-(8) and Figures (9)-(10) show predictions of the proposed simplified transient two-phase model for test cases 1-B and 1-C, respectively. Figure 7 shows the prediction of the proposed simplified transient two-phase model for pressure at test stations for test case 1-B. The figure also shows that the proposed model predicted experimental pressure data at ε_{ave} = −4.07% and ε_{ave} = −4.40% for initial (I) and final (F) flow conditions, respectively. Figure 8 shows a similar prediction for liquid holdup at ε_{ave} = 33.57% and ε_{ave} = 41.00%, for initial and final flow, respectively.

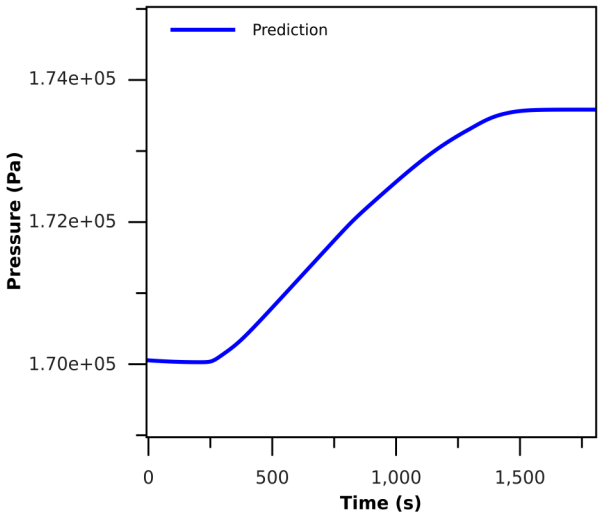

Figure 7. Simplified Transient Model Compared with Experimental Data [7] (pressure results for test 1-B)

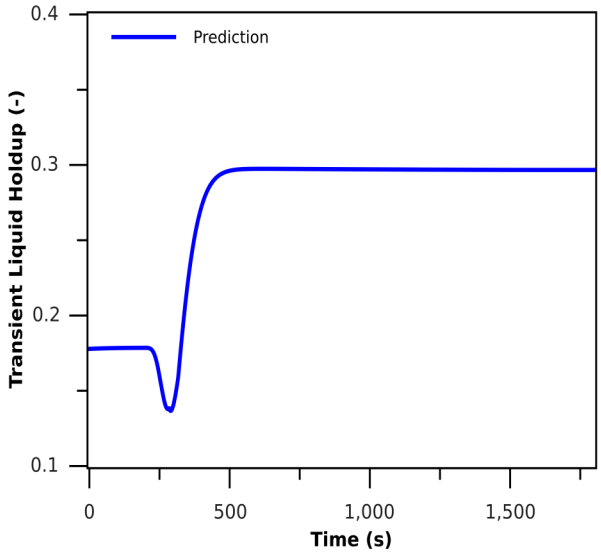

Figure 8. Simplified Transient Model (liquid holdup results for test 1-B)

Figure 9 shows the prediction of the proposed simplified transient two-phase model for pressure at test stations for test case 1-C. The result showed that the proposed simplified transient two-phase model predicts experimental pressure data at ε_{ave} = 1.91% and ε_{ave} = −3.32%, for initial (I) and final (F) flow conditions, respectively. Figure 10 shows a similar prediction for liquid holdup at ε_{ave} = −54.84% and ε_{ave} = −11.92%, for initial and final flow, respectively.

Conclusions

Based on the simplifications to the two-phase Navier-Stokes equations, a simplified transient two-phase model was obtained, which was capable of predicting pressure and liquid holdup.

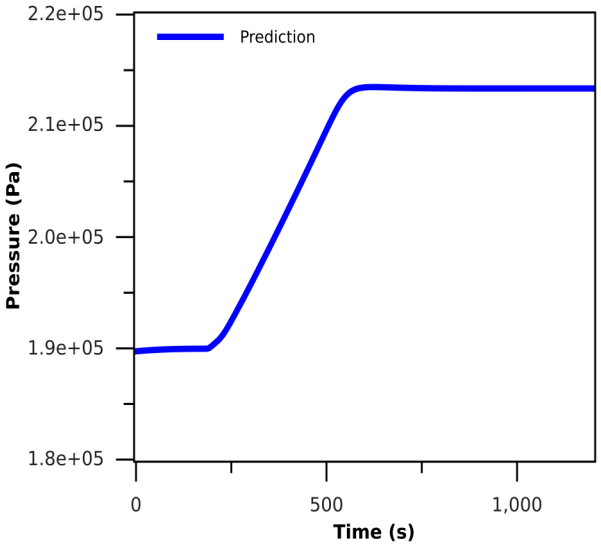

Figure 9. Simplified Transient Model (pressure results for test 1-C)

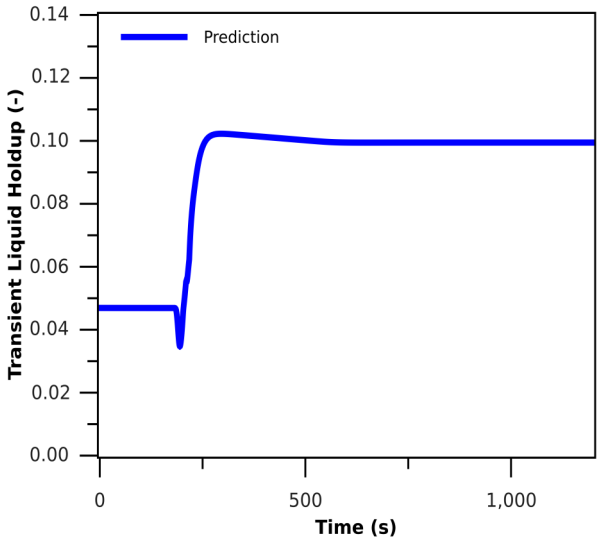

Figure 10. Simplified Transient Model Compared with Experimental Data [7] (liquid holdup results for test 1-C)

Nomenclature

α_G	=	Gas fraction [-]
α_L	=	Liquid fraction or transient liquid holdup [-]
β	=	Slope limiter to determine flow direction [-]
C_0	=	Coefficient of Bubble distribution in flow [-]
D	=	Internal diameter of pipe [m]
ε_{ave}	=	Average percentage error [%]
f_m	=	Friction factor of mixture flow in pipe [-]
g	=	Acceleration due to gravity [m/s^2]
H_L	=	Steady state liquid holdup [-]
λ_L	=	No-slip liquid holdup [-]
μ_G	=	Gas viscosity [Pa.s]
μ_L	=	Liquid viscosity [Pa.s]
v_L	=	Kinematic viscosity [m^2/s]
N	=	Number of elements in computational domain
$N+1$	=	Number of nodes in computational domain
P	=	Pressure [Pa]
P_G	=	Gas pressure [Pa]
P_L	=	Liquid pressure [Pa]
P_{sep}	=	Separator Pressure [bar]; 1 bar ≡ 100000 Pa
θ	=	Angular inclination of pipe [degree]
ρ_G	=	Gas density [Kg/m^3]
ρ_L	=	Liquid density [Kg/m^3]
ρ_m	=	Density of gas-liquid mixture [Kg/m^3]
Re	=	Reynolds number [-]
σ	=	Surface tension [N/m]
t	=	time [s]
t_{N+1}	=	computation time at N+1 pipe discretization [s]
t_{42}	=	computation time at 42 pipe discretization [s]
τ_{GW}	=	Gas-wall shear stress [Pa]
τ_{GL}	=	Gas-liquid interface shear stress [Pa]
τ_{LW}	=	Liquid-wall shear stress [Pa]
U_D	=	Drift velocity [m/s]
U_G	=	Gas velocity [m/s]
U_L	=	Liquid velocity [m/s]
U_m	=	Mixture velocity [m/s]
U_{SG}	=	Gas superficial velocity [m/s]
U_{SL}	=	Liquid superficial velocity [m/s]
x,L	=	Length [m]
Δt	=	time step [s]
Δx	=	spatial increment [m]

Superscript

n	=	Previous time step
n+1	=	Current time step
G	=	Gas
L	=	Liquid

Subscript

i	=	node of discretized pipe
j	=	element of discretized pipe

References

[1] Shoham, O. (2005). *Mechanistic modeling of gas-liquid two-phase flow in pipes*. Society of Petroleum Engineers.

[2] Brill, J. P. (1987). *Multiphase Flow in Wells*. Society of Petroleum Engineers.

[3] Prosperetti, A., & Tryggvason, G. (2007). *Computational Methods for Multiphase Flow*. Cambridge University Press.

[4] Taitel, Y., Shoham, O., & Brill, J. P. (1989). Simplified transient solution and simulation of two-phase flow in pipelines. *Chemical Engineering Science*, *44* (6), 1353–1359.

[5] Minami, K., & Shoham, O. (1994). Transient two-phase flow behavior in pipelines-experiment and modeling. *International Journal of Multiphase*, *20*(4), 739-752.

[6] Li., M. (2010, May). *Transient Two-Phase Flow Modeling*. In Seventy Sixth Semi-Annual Advisory Board Meeting Brochure and Presentation, Tulsa University Fluid Flow Projects.

[7] Vigneron, F., Sarica, C., & Brill, J. P. (1995, June). Experimental analysis of imposed two-phase flow transients in horizontal pipelines. *In the 7th International Conference, Multiphase* (pp. 199-217).

[8] Choi, J., Pereyra, E., Sarica, C., Lee, H., Jang, I. S., & Kang, J. (2013). Development of a fast transient simulator for gas–liquid two-phase flow in pipes. *Journal of Petroleum Science and Engineering*, *102*, 27-35.

[9] Bendiksen, K. H., Maines, D., Moe, R., & Nuland, S. (1991). The dynamic two-fluid model OLGA: Theory and application. *SPE Production Engineering*, *6* (02), 171-180.

[10] Garcıa, F., Garcıa, R., Padrino, J. C., Mata, C., Trallero, J. L., & Joseph, D. D. (2003). Power law and composite power law friction factor correlations for laminar and turbulent gas–liquid flow in horizontal pipelines. *International Journal of Multiphase Flow*, *29*(10), 1605-1624.

[11] Choi, J., Pereyra, E., Sarica, C., Park, C., & Kang, J. M. (2012). An efficient drift-flux closure relationship to estimate liquid holdups of gas-liquid two-phase flow in pipes. *Energies*, *5*(12), 5294-5306.

[12] Asante, B. (2000). *Multiphase Transport of gas and Low Loads of Liquids in Pipelines*. Unpublished doctoral dissertation, University of Calgary.

[13] Hernandez Perez, V. (2008). *Gas-liquid two-phase flow in inclined pipes*. Unpublished doctoral dissertation, University of Nottingham.

[14] Marruaz, K. S., Gonçalves, M. A., Ribeiro, G. S., França, F. A., & Rosa, E. S. (2001). Horizontal slug

flow in a large-size pipeline: experimentation and modeling. *Journal of the Brazilian Society of Mechanical Sciences*, *23*(4), 481-490.

[15] Tullius, L. (2000). *A study of drag reducing agents in multiphase flow in large diameter horizontal pipelines*. Unpublished doctoral dissertation, Ohio University.

Biographies

OLUSOLA OLORUNTOBA received his MSc degree in Offshore and Ocean Technology from Cranfield University in 2012. His areas of research are related to subsea engineering, flow assurance, and computational modeling. Olusola may be reached at o.a.oloruntoba@cranfield.ac.uk

FUAT KARA is a lecturer at Cranfield University. Fuat's research areas are related to subsea engineering, pipeline engineering, fluid-structure interaction, marine hydrodynamics, marine hydroelasticity, and offshore renewable energy systems (offshore wind, wave, and tidal devices). Fuat may be reached at f.kara@cranfield.ac.uk